

## SUPPLEMENTARY EXPERIMENTAL PROCEDURES

### Mice

C57BL/6, *Rag1*<sup>-/-</sup>, *Tcrd*<sup>-/-</sup> and *muMt*<sup>-/-</sup> mice were purchased from The Jackson laboratory (Bar Harbor, ME). Mice were maintained under specific pathogen-free (SPF) conditions at the Icahn School of Medicine at Mount Sinai. The generation of IL23 conditional knock-in mice (*R23* mice and *R23FR* mice) is detailed in Supplementary Figure 1. All the germ-free (GF) mice were bred in-house and housed in standard flexible film isolators in our GF animal facility. All animal experiments were performed in accordance with the approved guidelines for animal experimentation at the Icahn School of Medicine at Mount Sinai.

### Diet Treatment

All mice were raised on the basal diet 5053, which was purchased from LabDiet (St. Louis, MO). The basal diet 2019 (TD. 160647) was purchased from Envigo (Madison, WI). Tamoxifen (TAM) (500mg/kg) (Sigma) was added to the Envigo diet 2019 (TD.130968). *R23FR* mice and control *FR* mice were fed with tamoxifen diet during the indicated times shown as Figure 1A. After each cycle of TAM treatment, animals were switched back to the basal diet 5053.

### Quantification of Fecal Lcn-2 by Enzyme-linked Immunosorbent Assay (ELISA)

Freshly collected or frozen fecal samples were reconstituted in PBS containing 0.1% Tween 20 (100 mg/ml) and vortexed for 20 min to get a homogenous fecal suspension<sup>1</sup>. These samples were then centrifuged for 10 min at 12,000 rpm and 4°C. Clear supernatants were collected and stored at -20°C until analysis. Lcn-2 levels were estimated in the supernatants using DuoSet murine Lcn-2 ELISA kit (R&D Systems, Minneapolis, MN).

### Histology

Tissues were dissected, fixed in 10% phosphate-buffered formalin, and then processed for paraffin sections. Five-micrometer sections were stained with hematoxylin and eosin (H&E) for histological analyses. All the sections were evaluated for a wide variety of histological features that included epithelial integrity, number of goblet cells (mucin production), stromal inflammation, crypt abscesses, erosion, and submucosal edema. Severity of disease was then classified based on a modified version of the Histologic Activity Index as described before<sup>2</sup>. Briefly, the disease score in the large intestine was calculated as follows: grade 0: absence of epithelial damage, focal stromal inflammation or regenerative changes; grade 1: crypt abscesses in less than 50% of the epithelium. Diffuse stromal inflammation and/or regenerative changes; grade 2: crypt abscesses in more than 50% of the epithelium and focal erosion or cryptic loss. Diffuse and accentuated crypt distortion with stromal inflammation; grade 3: Pan-colitis, diffuse erosion and ulcers.

#### Intraperitoneal Injection of Recombinant IL23

*R23FR* mice after TAM treatment for 49 days were injected intraperitoneally (i.p.) with 2 $\mu$ g recombinant mouse IL23 (R&D System) per mouse. Injections were continued in this manner every other day for 3 times (days 49, 51, and 53). Mice were sacrificed at d56, and gut was taken for histological analysis (Supplementary Figure 5).

#### Antibodies

For flow cytometry, the following fluorochrome-conjugated anti-mouse antibodies were used: CD45 (30-F11), CD3e (145-2C11), CD4 (GK1.5), CD8a (53-6.7), CD11b (M1/70), CD11c (N418), F4/80 (BM8), Ly6C (HK1.4), NK1.1 (PK136), NKp46 (29A1.4), CD19 (eBio1D3), CD117 (2B8), CD127 (A7R34) were from eBioscience; Siglec-F (E50-2440) was from BD Biosciences; Ly6G (1A8)

and anti-mouse Lineage Cocktail with Isotype Ctrl was from Biolegend; IL-33R (T1/S2, clone DJ8) from MD Bioproducts.

### Flow Cytometry and Sorting

Cell suspensions from the *lamina propria* and mLN were prepared as described previously<sup>3</sup>. All cells were first pre-incubated with anti-mouse CD16/CD32 for blockade of Fc  $\gamma$  receptors, then were washed and incubated for 30 min with the appropriate monoclonal antibody conjugates in a total volume of 200  $\mu$ l PBS containing 2 mM EDTA and 2% (vol/vol) bovine serum. 4,6-diamidino-2-phenylindole (DAPI) (Invitrogen) was used to distinguish live cells from dead cells during cell analysis and sorting. Stained cells were analyzed on a LSRII machine using Diva program (BD Bioscience) and data were analyzed with FlowJo software (TreeStar). Stained CD4<sup>+</sup> T cells (DAPI<sup>-</sup>CD45<sup>+</sup>CD3<sup>+</sup>CD4<sup>+</sup>CD8<sup>-</sup>) were purified with a MoFlo Astrios cell sorter (DakoCytomation). Cells were > 95% pure after sorting. The sorted CD4 T cells were used for TCR sequencing. Stained intestinal YFP<sup>+</sup> (DAPI<sup>-</sup>CD45<sup>+</sup>YFP<sup>+</sup>) and YFP<sup>-</sup>CD11b/c<sup>+</sup> (DAPI<sup>-</sup>CD45<sup>+</sup>YFP<sup>-</sup>CD11b/c<sup>+</sup>) populations were purified with a MoFlo Astrios cell sorter and used for qPCR analysis of IL23 mRNA expression.

### T cell Purification

For CD4<sup>+</sup> T-cell isolation, mLNs and large intestine were digested in collagenase as described previously<sup>3</sup>. CD4<sup>+</sup> T cells were enriched by positive immunoselection using CD4-(L3T4) microbeads (Miltenyi Biotec). The magnetic-activated cell sorting (MACS) purified CD4<sup>+</sup> T cells were used as donor cells in adoptive transfer experiments.

### Microbiota Transplantation

Cecal extracts pooled from 3-5 donor SPF mice were suspended in PBS (2.5 ml per cecum) and were administered (0.1 ml per mouse) immediately to *R23FR* and *FR* germ-free mice that were generated in house<sup>4</sup>. Transplanted mice were maintained in separate filter-top gnotobiotic cages and two weeks after were used for the further experiments<sup>5</sup>.

#### DNA Extraction, 16S rDNA Amplification, and Multiplex Sequencing

DNA was obtained from feces of mice using a bead-beating protocol<sup>6</sup>. Briefly, mouse fecal pellets (~50 mg), were re-suspended in a solution containing 700 $\mu$ L of extraction buffer [0.5% SDS, 0.5 mM EDTA, 20 mM Tris-Cl] and 200 $\mu$ L 0.1-mm diameter zirconia/silica beads. Cells were then mechanically disrupted using a bead beater (BioSpec Products, Bartlesville, OK; maximum setting for 5 min at room temperature), followed by extraction with QIAquick 96 PCR Purification Kit (Qiagen). Bacterial 16S rRNA genes were amplified using the primers as previously described<sup>7</sup>. Sample preparation and analysis of 16S rDNA sequence were done as previously described<sup>8</sup>. The 16S rDNA data were analyzed with MacQIIME 1.9.1. Operational taxonomic units (OTUs) were picked with 97% sequence similarity and the sequences were aligned to the Greengenes closed reference set with a minimum sequence length of 150bp and a minimum percent identity of 75%<sup>9,10</sup>.

#### Antibiotic Treatment

For reduction of the intestinal microbiota, a 'cocktail' of antibiotics containing ampicillin 1g/L, metronidazole 1g/L, neomycin 1g/L, and vancomycin 0.5g/L (Sigma Aldrich) in the drinking water was provided to the mice through their drinking water. Antibiotic treatment was renewed every week.

### Reverse-transcription Polymerase Chain Reaction

Total RNA from tissues/sorted cells was extracted using the RNeasy mini/micro Kit (Qiagen) according to the manufacturer's instructions. Complementary DNA (cDNA) was generated with Superscript III (Invitrogen). Quantitative PCR (qPCR) was performed using SYBR Green Dye (Roche) on the 7500 Real Time System (Applied Biosystems) machine. Thermal cycling conditions used were as follows: 50 °C for 2min and 95 °C for 10 min, 40 cycles of 95 °C for 15 s, 60 °C for 1min, followed by dissociation stage. Results were normalized to the housekeeping gene Ubiquitin (Ubi). Relative expression levels were calculated as  $2^{(Ct(\text{Ubiquitin})-Ct11)}$ . Primers were designed using Primer3Plus<sup>12</sup>.

### In Vivo Antibody Treatment

To deplete CD4<sup>+</sup> and CD8<sup>+</sup> cells in mice, *R23FR* mice treated with TAM were administered 100µg anti-CD4 (GK1.5, BioXcell) or anti-CD8 (53-5.8, BioXcell) or isotype antibodies (rat IgG2b, LTF-2; rat IgG1, TNP6A7; Both from BioXcell) intravenously at day 48, 49, 50, 52 and 54. Mice were sacrificed at day 56, and large intestine was taken for histological analysis (Figure 5).

### T cell Adoptive Transfer

One million CD4<sup>+</sup> from mLN and/or large intestine enriched by using MACS-beads (Miltenyi Biotech) were transferred into *Rag1*<sup>-/-</sup> recipient mice by intravenous (i.v.) injection.

### Bulk Sequencing of TCRs


Briefly, cells were suspended in Trizol (Invitrogen) and total RNA was isolated. Using poly T beads, mRNA was isolated and fragmented briefly to generate 600-800bp fragments by using mRNA-seq kit (Bioo Scientific Corporation). Each of these RNA fragments were then converted

to double stranded cDNA using random primers, end repaired and an A base added to each 3'end of the fragment. Two universal DNA sequences (A and B) (compatible with Illumina sequencing instruments) were ligated to each end of the fragment respectively. To enrich the library for T cell receptor transcripts, two sets of PCR reactions were performed. The first PCR reaction was done using a primer complementary to the Constant region and the universal sequence A. The second, nested PCR was performed using another constant region primer and universal sequence A. In the end Illumina compatible amplicons were generated with greater than 90% specificity to the T cell receptor transcripts.

The unique molecular indexes (UMID) in the sequenced reads were used to remove PCR duplicates and the reads were mapped to annotated V and J segments, which are compiled from IMGT (<http://www.imgt.org>), genome annotations from USUC (<http://genome.ucsc.edu>) and data from previous sequencing experiments performed in-house. All sequences that unambiguously mapped to V and J segments were translated to amino-acid sequences, in all three frames. Complementary determining region 3 (CDR3) sequences have well-defined boundaries, which were used to identify the CDR3 fragments in the translated open reading frames. Various categories (V-J pairs, CDR3 sequences, V-CDR3-J combinations) were tabulated from the data. Clonally expanded alpha and beta CDR3 were identified from the data, and the samples were clustered on the basis of the categories.

#### Statistical Analysis

All statistical analyses were performed with GraphPad Prism 5 software. Differences between groups were analyzed with Student's *t* tests or nonparametric Mann-Whitney test. Statistical tests are indicated throughout the Figure legends. Differences were considered significant when

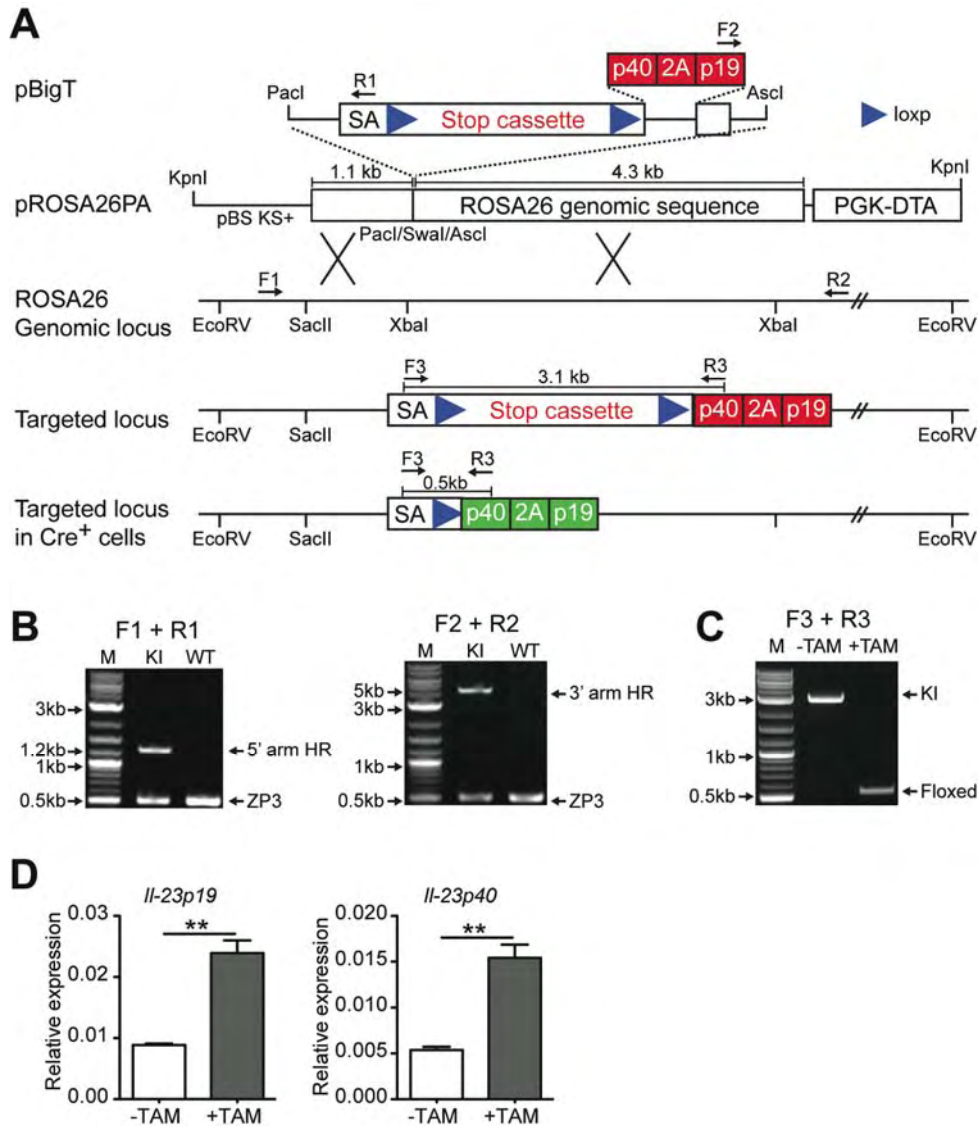


$p < 0.05$  (NS, not significant, \*  $p < 0.05$ , \*\* $p < 0.01$ , \*\*\* $p < 0.001$ ), and levels of significance are specified throughout the Figure legends. Data are shown as mean values  $\pm$  SEM throughout.

## REFERENCES FOR SUPPLEMENTARY EXPERIMENTAL PROCEDURES

1. Chassaing B, Srinivasan G, Delgado MA, et al. Fecal lipocalin 2, a sensitive and broadly dynamic non-invasive biomarker for intestinal inflammation. *PLoS One* 2012;7:e44328.
2. Gupta RB, Harpaz N, Itzkowitz S, et al. Histologic inflammation is a risk factor for progression to colorectal neoplasia in ulcerative colitis: A cohort study. *Gastroenterology* 2007;133:1099-1105.
3. He Z, Chen L, Souto FO, et al. Epithelial-derived IL-33 promotes intestinal tumorigenesis in *Apc* (Min/+) mice. *Sci Rep* 2017;7:5520.
4. Vijay-Kumar M, Aitken JD, Carvalho FA, et al. Metabolic syndrome and altered gut microbiota in mice lacking Toll-like receptor 5. *Science* 2010;328:228-31.
5. Faith JJ, Ahern PP, Ridaura VK, et al. Identifying Gut Microbe-Host Phenotype Relationships Using Combinatorial Communities in Gnotobiotic Mice. *Science Translational Medicine* 2014;6.
6. Ridaura VK, Faith JJ, Rey FE, et al. Gut microbiota from twins discordant for obesity modulate metabolism in mice. *Science* 2013;341:1241214.
7. Faith JJ, Guruge JL, Charbonneau M, et al. The long-term stability of the human gut microbiota. *Science* 2013;341:1237439.
8. Bongers G, Pacer ME, Geraldino TH, et al. Interplay of host microbiota, genetic perturbations, and inflammation promotes local development of intestinal neoplasms in mice. *J Exp Med* 2014;211:457-72.
9. Caporaso JG, Bittinger K, Bushman FD, et al. PyNAST: a flexible tool for aligning sequences to a template alignment. *Bioinformatics* 2010;26:266-7.
10. McDonald D, Price MN, Goodrich J, et al. An improved Greengenes taxonomy with explicit ranks for ecological and evolutionary analyses of bacteria and archaea. *ISME J* 2012;6:610-8.
11. Burton PR, Clayton DG, Cardon LR, et al. Genome-wide association study of 14,000 cases of seven common diseases and 3,000 shared controls. *Nature* 2007;447:661-678.
12. Untergasser A, Nijveen H, Rao X, et al. Primer3Plus, an enhanced web interface to Primer3. *Nucleic Acids Res* 2007;35:W71-4.

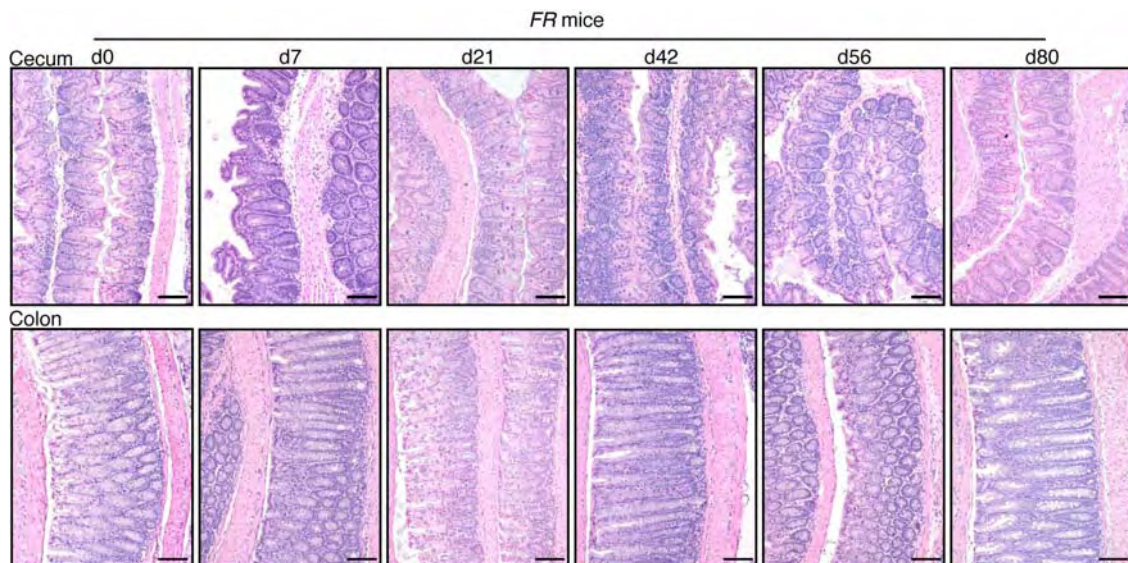




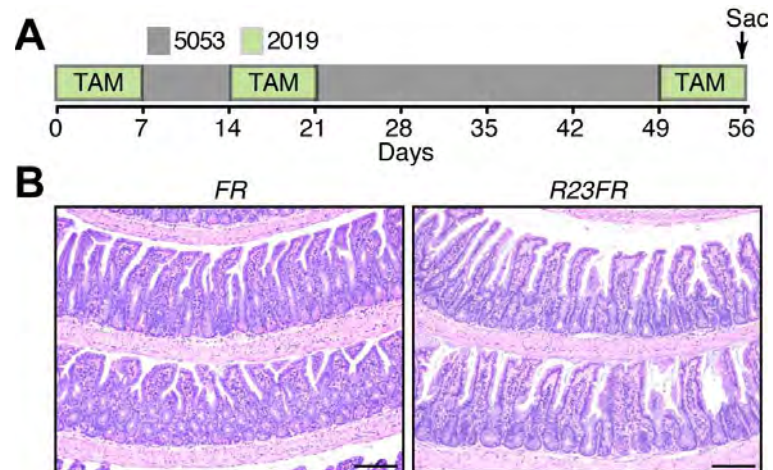
**Supplementary Figure 1.** Generation and validation of conditional IL23 knock-in mice. (A) IL23p40-2A-IL23p19 sequences were cloned into the pBigT plasmid containing a loxP-flanked STOP cassette containing a PGK-neo selectable marker and a tpA sequence (top). Schematic representation of the targeting strategy used to flank stop cassette with loxP sites (middle) and excision with Cre-recombinase (bottom). (B) Properly R23 recombined ES cell clones were identified by PCR analysis using diagnostic primers located outside the area of homology (F1+R1 and F2+R2 primer pairs). KI, knock-in clone; WT, wild type clone. The amplification of ZP3 was used as PCR internal control. (C) PCR detection of undeleted and deleted floxed alleles in R23FR mice without or with TAM treatment using primer set F3 and R3 against of genomic DNA from sorted YFP<sup>+</sup> (CX3CR1<sup>+</sup>) cells. A 3100-bp product corresponding to the non-deleted floxed allele was amplified by primers F3 and R3 from untreated R23FR mice DNA, whereas a 500-bp fragment corresponding to the deleted allele was amplified from treated R23FR mice.

---

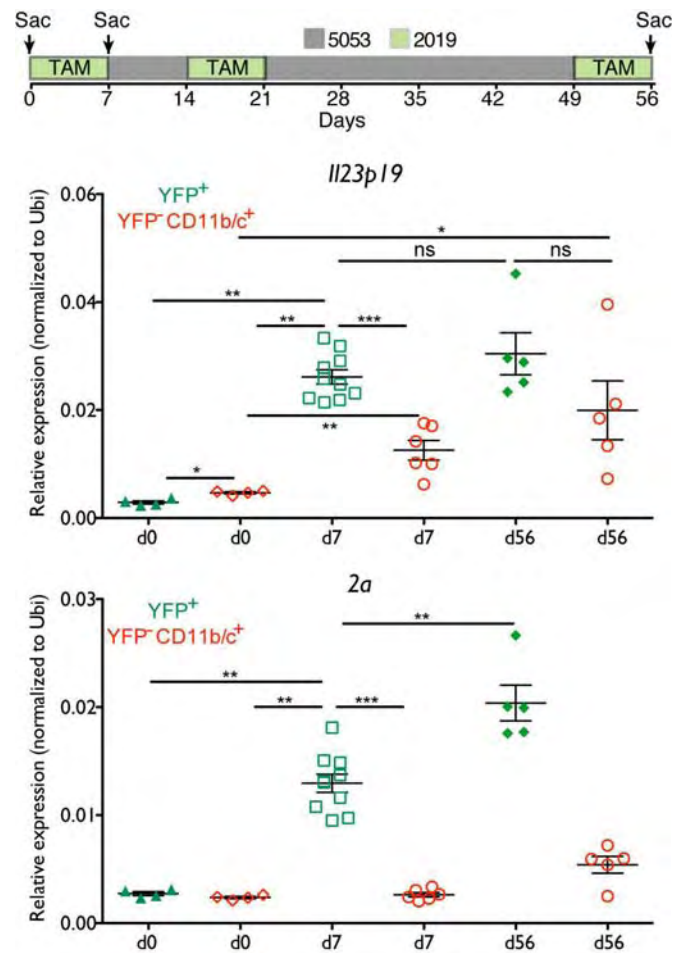
(D) qPCR analysis of IL23p19 and p40 mRNA expression from sorted YFP<sup>+</sup> (CX3CR1<sup>+</sup>) cells from large intestine of *R23FR* mice without or with TAM treatment for 7 days. Columns and bars represent mean  $\pm$  s.e.m (\*\*p<0.01, Mann-Whitney test).



**Supplementary Figure 2.** Histology of large intestine from control *FR* mice after TAM treatment. Histological analysis of treated *FR* mice did not show any abnormalities at any time points. Images of representative H&E-stained cecum and colon sections of *FR* mice at different time points after TAM treatment. Scale bars, 100  $\mu$ m.



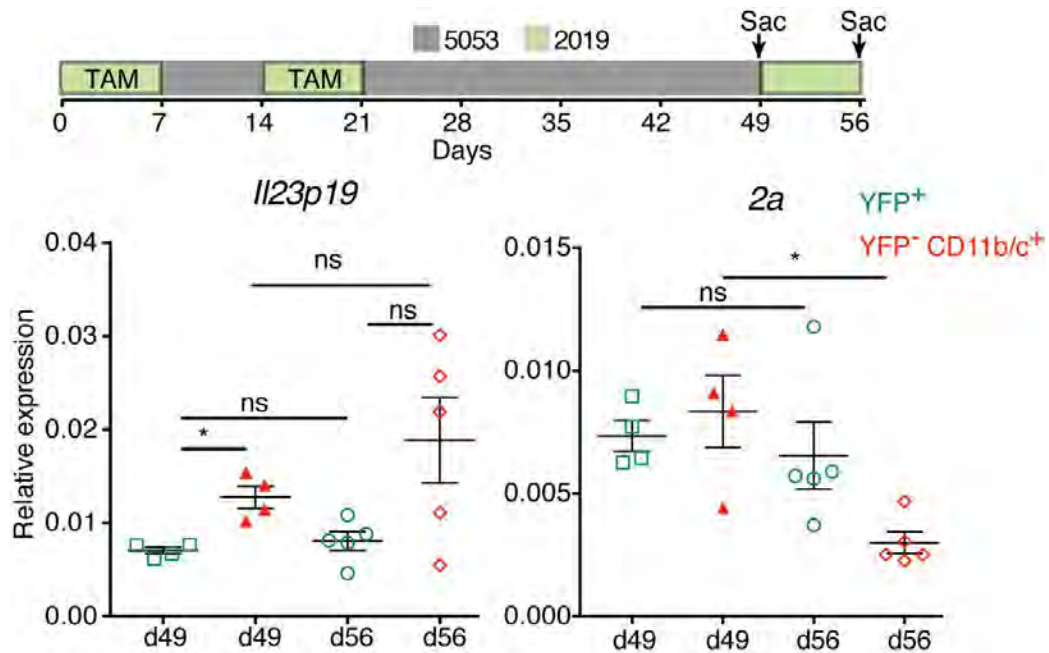
**Supplementary Figure 3.** The small intestine of *R23FR* and *FR* mice do not show gross abnormalities after TAM treatment. (A) Tamoxifen (TAM) in diet 2019 (green) was fed to *R23FR* and *FR* mice during the indicated times. After each cycle of TAM treatment, animals were switched to our mouse facility diet 5053 (gray). (B) Images of representative H&E-stained SI sections of *R23FR* and *FR* mice at d56 after TAM treatment. Scale bars, 100  $\mu$ m.



**Supplementary Figure 4.** TAM administration induces IL23 mRNA expression in the gut of *R23FR* mice at different time points. Tamoxifen (TAM) in diet 2019 (green) was fed to *R23FR* mice during the indicated times. After each cycle of TAM treatment, animals were switched to our mouse facility diet 5053 (gray). FACS sorted *R23FR* cecum *YFP<sup>+</sup>* and *YFP<sup>-</sup>CD11b/c<sup>+</sup>* populations were used for qPCR analysis of IL23 expression at d0, d7 and d56. Gene expression as profiled by q-PCR is shown for *2a* and *Il23p19*. \* $p < 0.05$ , \*\* $p < 0.01$ , \*\*\* $p < 0.001$ , ns, not significant; by nonparametric Mann-Whitney test.

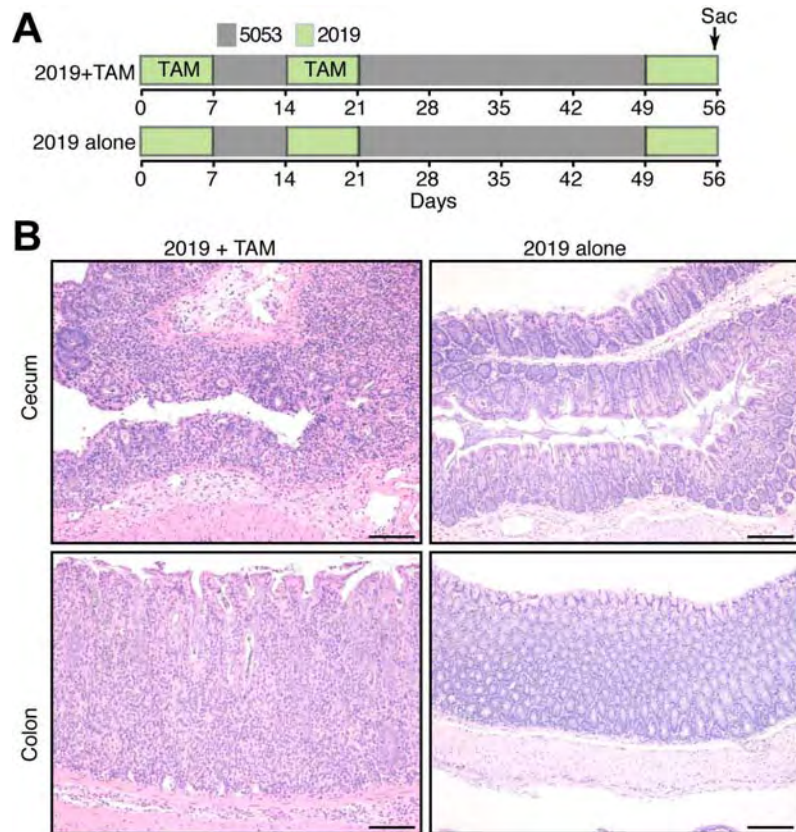




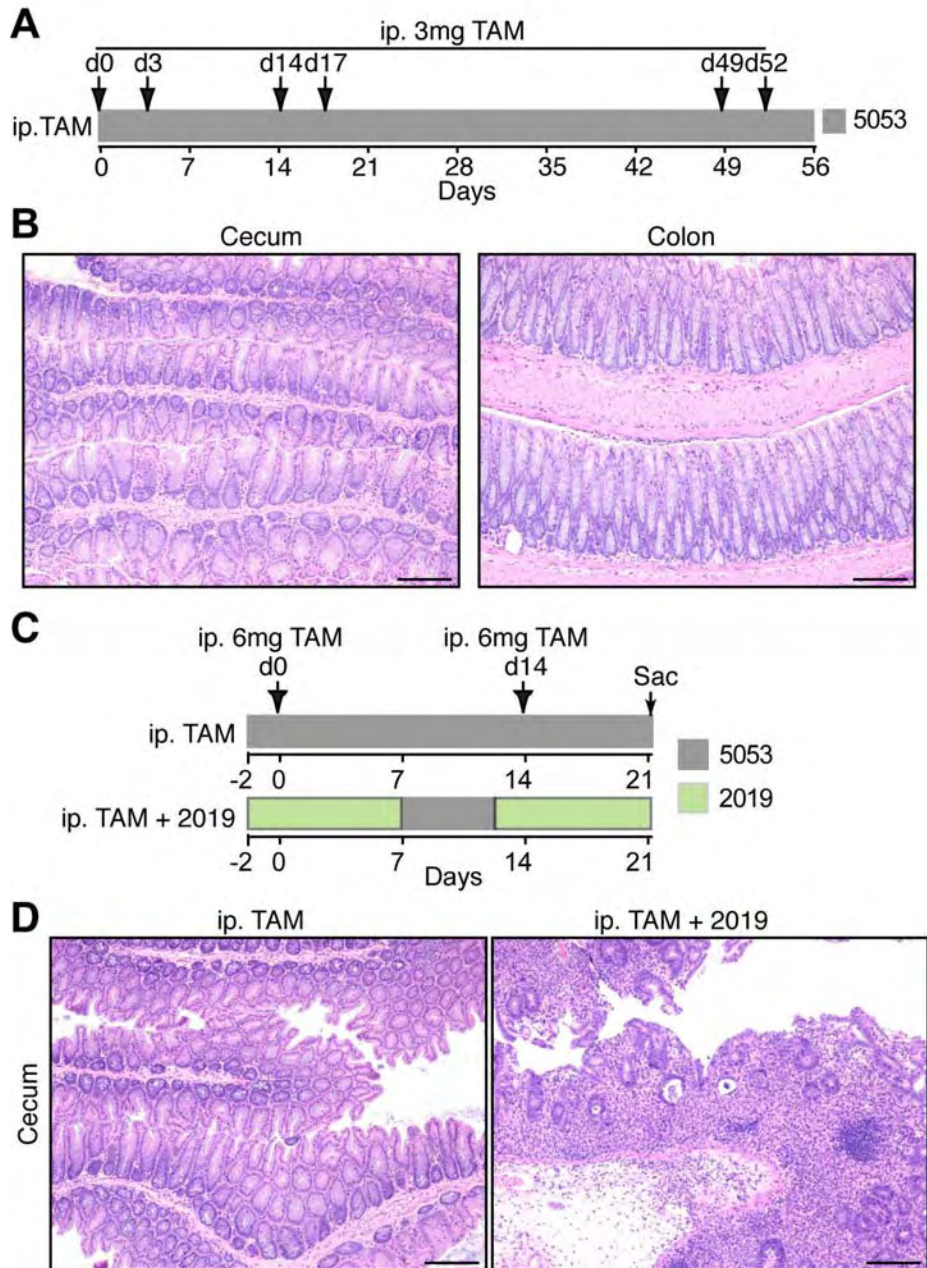


**Supplementary Figure 6.** IL23 mRNA expression in the cecal myeloid populations in *R23FR* mice at remission and relapse stages. Gene expression as profiled by q-PCR is shown for *2a* and *Il23p19*. \* $p < 0.05$ , ns, not significant; by nonparametric Mann-Whitney test. Notice that there were no differences in the expression of *2a* and *Il23p19* between the remission stage (d49) and relapse stage (d56) regardless of the cell population analyzed (YFP<sup>+</sup> and YFP<sup>-</sup>CD11b/c<sup>+</sup> populations).

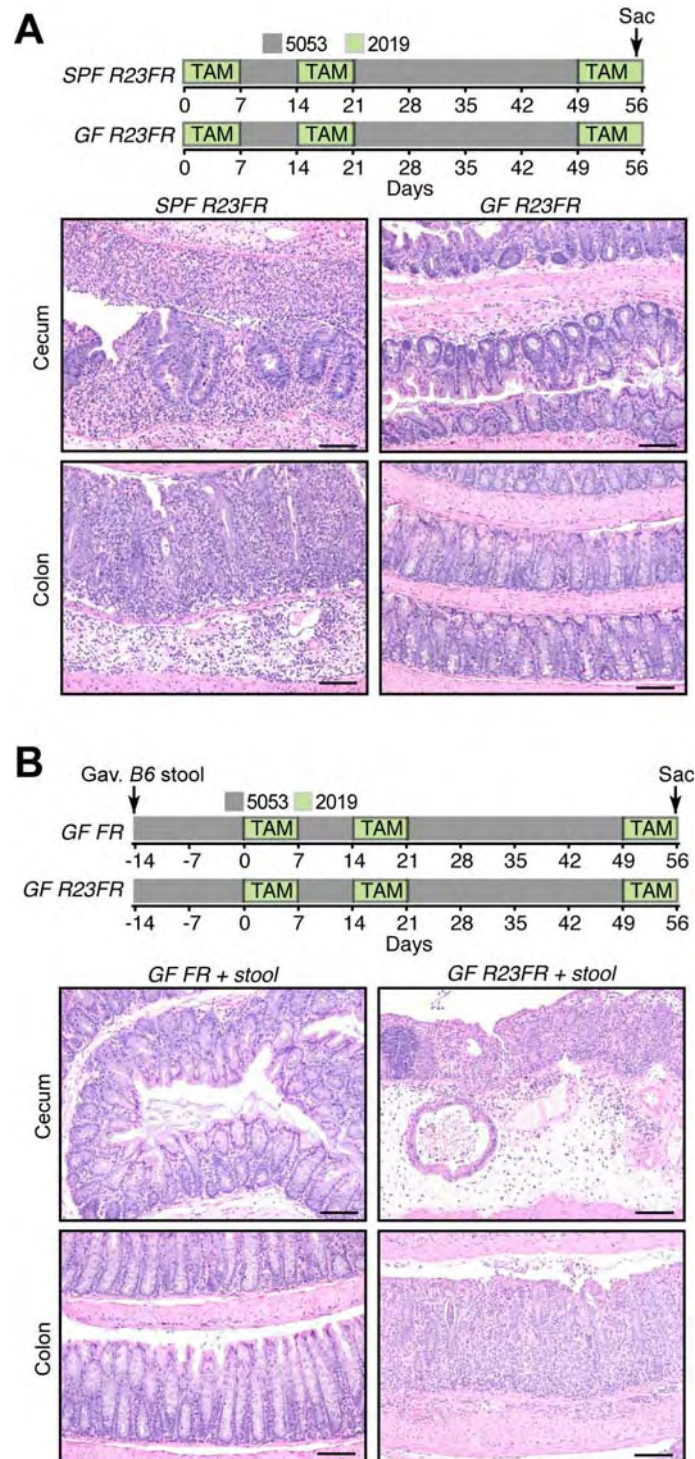




**Supplementary Figure 7.** Treatment of *R23FR* mice with repeated cycles of diet 2019 does not elicit colitis. (A) Schematic representation depicts the experimental design used to test if diet 2019 alone could induce colitis. (B) Representative H&E-stained cecum and colon sections of *R23FR* mice treated with the conventional 3 cycles of diet 2019 + TAM or treated with 3 cycles of diet 2019. Administration of diet 2019 to *R23FR* mice using the 3 cycles paradigm did not elicit disease. Scale bars, 100  $\mu\text{m}$ .



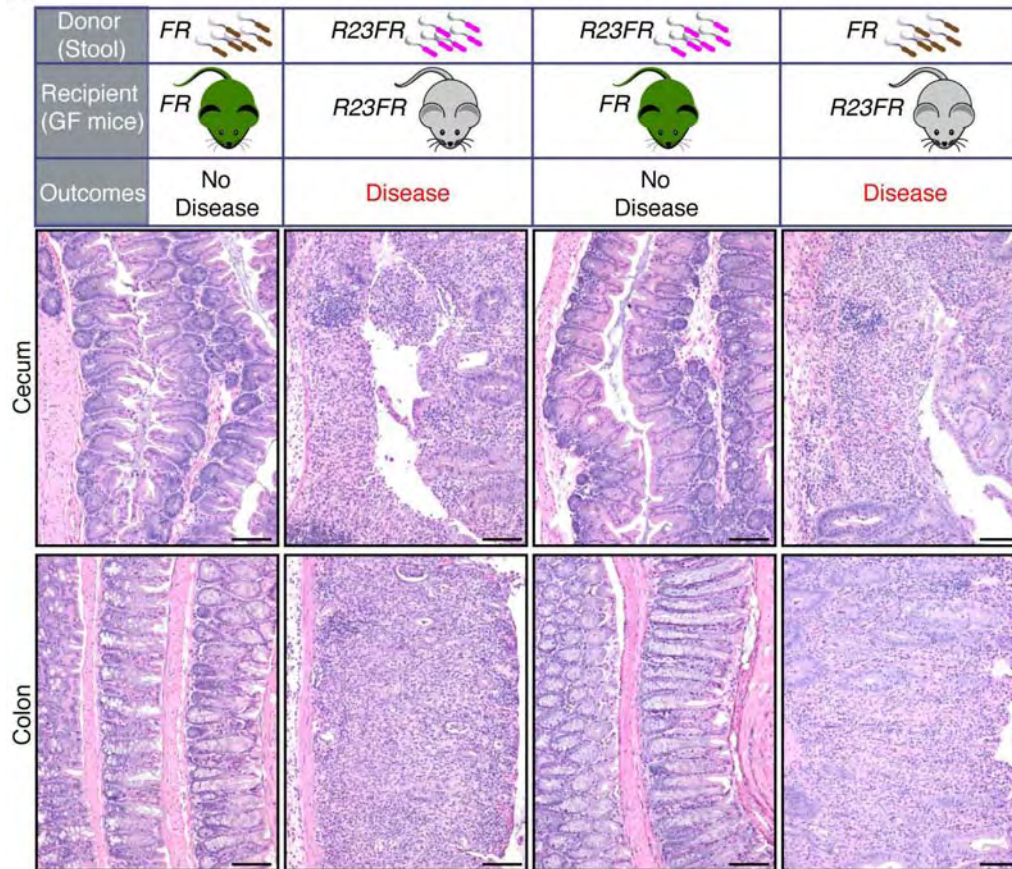
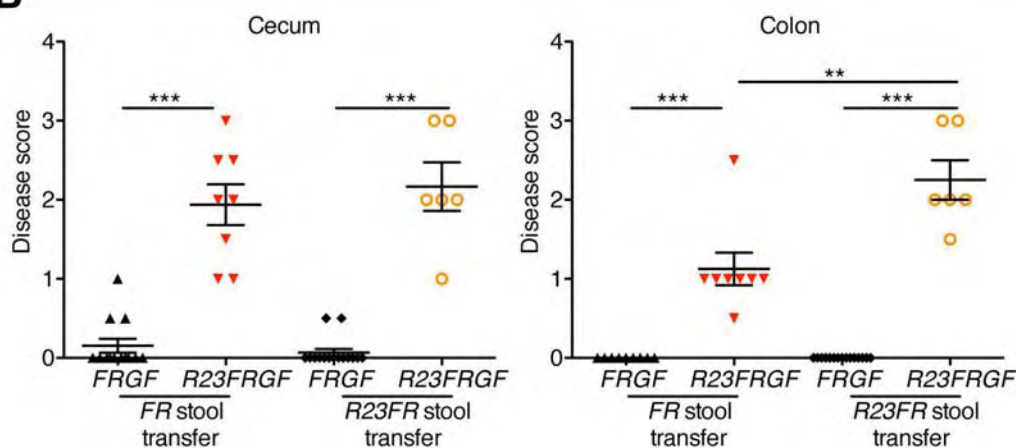
Supplementary Figure 8. Different disease outcomes in mice injected i.p. with TAM. (A) *R23FR* mice were treated with i.p. TAM to mimic the 3 weekly cycles and sacrificed at day 56 as indicated. (B) Representative H&E-stained sections of cecum and colon ( $n = 3$ ). Scale bars, 100  $\mu\text{m}$ . No disease was observed in the cecum or colon of the animals analyzed. (C) *R23FR* mice were injected with TAM i.p., and fed continuously with diet 5053, or two cycles of diet 2019, and sacrificed at d21 ( $n=3-4/\text{group}$ ). (D) Representative H&E-stained sections of cecum ( $n = 3/\text{group}$ ). Scale bars, 100  $\mu\text{m}$ . Notice absence of disease in mice treated with diet 5053, and marked colitis in animals treated with TAM i.p. and subjected to a diet switch.



**Supplementary Figure 9.** Microbiota is required for IL23-induced colitis. (A) SPF *R23FR* and GF *R23FR* mice were treated with TAM and sacrificed at day 56 as indicated (top). Representative H&E-stained sections of cecum and colon from SPF *R23FR* and GF *R23FR* mice ( $n = 5/\text{group}$ ) (bottom). Scale bars, 100  $\mu\text{m}$ . (B) Cecal contents from C57BL/6J mice

---

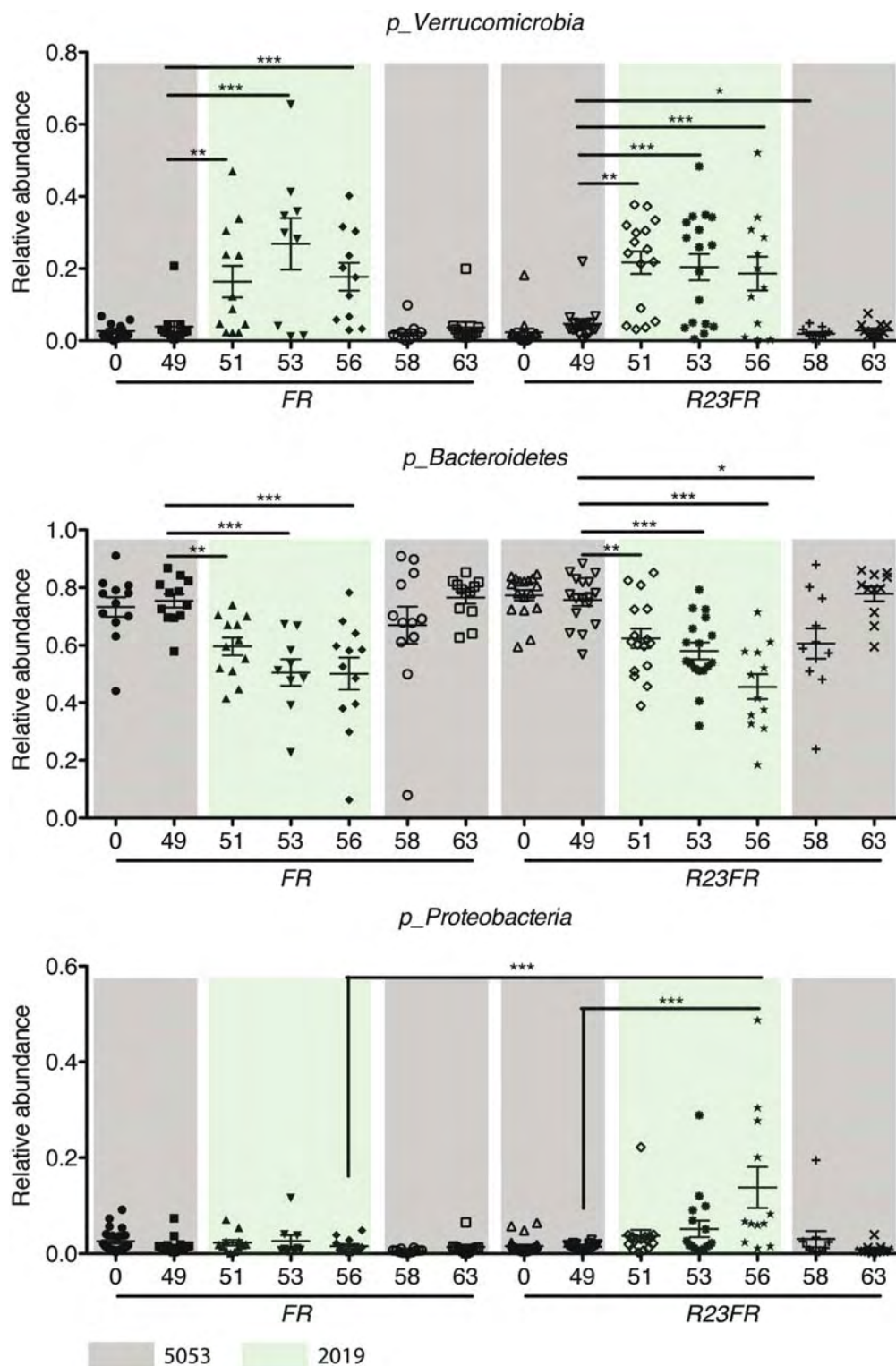
were transplanted via gavage into GF *FR* and GF *R23FR* mice following TAM treatment (top). Images of representative H&E-stained cecum and colon sections of GF *FR* and GF *R23FR* mice transplanted with stools (n = 5/group). Scale bars, 100  $\mu$ m.

**A****B**

**Supplementary Figure 10.** Transplantation of microbiota from R23FR and FR mice. (A) Cartoon depicts experimental design for the microbiota transfer experiments (top), the summaries of outcomes (middle), and representative H&E stained sections (bottom). Scale bars, 100  $\mu$ m. (B) Histological scores of the colon and cecum of germ-free R23FR

---

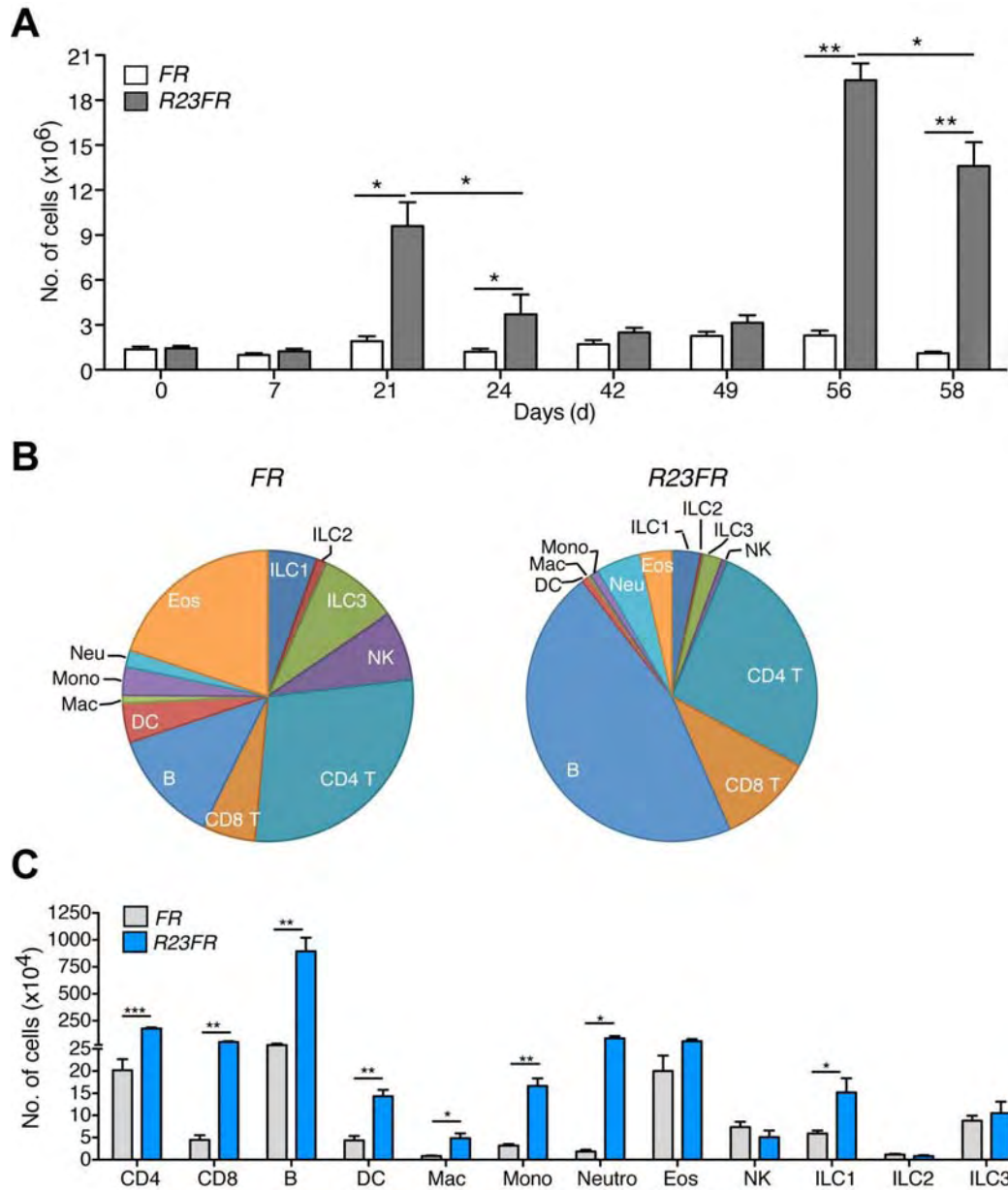
*and FR* mice transplanted with different donor stool. \*\* $p < 0.01$ , \*\*\*  $p < 0.001$ ; by nonparametric Mann-Whitney test.



**Supplementary Figure 11.** Changes in relative bacterial abundance over time in mice. Dot plot of relative abundance of *Verrucomicrobia*, *Bacteroidetes* and *Proteobacteria* in

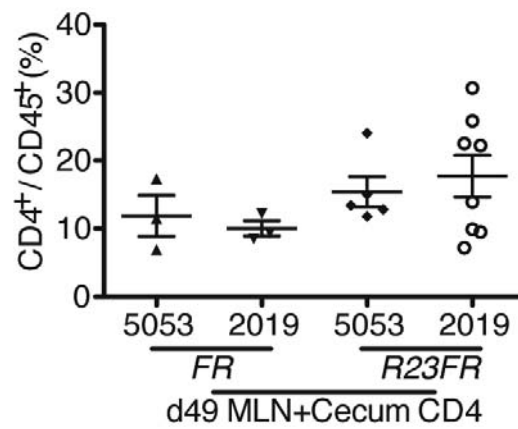
*R23FR* mice and *FR* mice in a longitudinal study of 16S rDNA sequencing. \* $p < 0.05$ , \*\* $p < 0.01$ , \*\*\*  $p < 0.001$ ; by nonparametric Mann-Whitney test.





**Supplementary Figure 12.** Expression of IL23 promotes changes in the number of leukocytes in the cecum. (A) Total CD45<sup>+</sup> cells in the cecum of *R23FR* and *FR* mice at different time points. (B-C) Relative (B) and absolute (C) number of lymphocytes, myeloid cells and innate lymphoid cells (ILC) are shown (n=3 mice/group) of *R23FR* and *FR* mice at day 56. Mean  $\pm$  s.e.m. \*p<0.05, \*\*p<0.01, \*\*\* p<0.001; by *t* test.





**Supplementary Figure 14.** Reconstitution of T cells subsets in Rag deficient mice. FACS analysis of CD4<sup>+</sup> T cells in the blood of recipient *Rag*<sup>-/-</sup> mice injected with CD4<sup>+</sup> T cells fed with distinct diets. There were comparable frequencies of CD4<sup>+</sup> T cells in the blood of the recipients after adoptive transfer of CD4<sup>+</sup> T cells. There were no significant differences between-group by student *t* test.

**Supplementary Table 1:** Definitions of clonotype groups classified according to frequency.

<b>Clone Type</b>	<b>Clone Size</b>
Rare	Single cell events
Small	More than single event, but less than 0.001%
Medium	From 0.001% to 0.01%
Large	From 0.01% to 1%
Hyperexpanded	More than 1%

**Supplementary Table 2:** The TCR $\alpha$  CDR3 aa sequence of the hyper-expanded clones in each sample (Related to Figure 7D)

Recipient Rag_2019_1		Recipient Rag_2019_2		Recipient Rag_2019_3		Recipient Rag_5053	
CDR3	%	CDR3	%	CDR3	%	CDR3	%
AAERANTNKVV	4.33	SASPNYAQGLT	4.07	ALSDRANYNVLY	4.78	AVSGNNAGAKLT	1.61
SASNYYAQGLT	3.35	AAERANTNKVV	3.22	ALSDPTGGYKVV	3.71	AAESGNYKYV	1.26
AAEGAGAKLT	2.06	ALSDRANYNVLY	3.19	AMRGGGSALGRLH	3.46	AMERGSNNRIF	1.23
AAGSNNRIF	2.03	AMRGGGSALGRLH	2.57	AAISSNTNKVV	3.46		
AVSAKSGGSNYKLT	1.32	ALSDPTGGYKVV	2.28	AVGTNSAGNKLT	3.33		
ALSDRANYNVLY	1.29	AASLSNYNVLY	2.14	AAERANTNKVV	1.98		
AMGGSNYKLT	1.21	ALSDWGNVLI	1.35	AVSAGGSNYKLT	1.42		
		AVSAKSGGSNYKLT	1.06	SASPNYAQGLT	1.27		
				AVSAKSGGSNYKLT	1.01		

Red: Shared clones in all three 2019 samples;

Blue: Shared clones in two 2019 samples;

Black: Unique clones in each samples.

**Supplementary Table 3:** The TCR $\beta$  CDR3 aa sequence of the hyper-expanded clones in each sample (Related to Figure 7D)

Recipient Rag_2019_1		Recipient Rag_2019_2		Recipient Rag_2019_3		Recipient Rag_5053	
CDR3	%	CDR3	%	CDR3	%	CDR3	%
ASGGGDRADTQY	5.21	ASGGGDRADTQY	4.52	ASSRDRGHSDYT	7.02	ASSFPGAEQF	2.28
ASSFYRAEQF	2.93	ASSRTGGYAEQF	3.76	ASSDRGAETLY	4.65	ASSAPNSDYT	2.05
ASSWRQKDTQY	2.33	ASSPPGNYAEQF	2.77	ASSQEPDWGLYEQY	3.52	ASSQVGSSYEQY	1.52
ASGDPTTNTVEF	2.27	ASRYWGGADTLY	1.39	ASGGGDRADTQY	2.16	AWTGGEEQY	1.05
ASSPGQGRKEDTQY	2.26	ASSLSWGGYAEQF	1.11	ASRYWGGADTLY	1.19		
ASRLGEGAETLY	1.99	ASSLTGDSPLY	1.06	ASSPPGNYAEQF	1.15		
ASRYWGGADTLY	1.73	ASSREGRNYAEQF	1.01	GALGVYEQY	1.13		
ASSPYTLY	1.56						
ASSFQGNSDYT	1.27						
ASSSTGVDTQY	1.05						
AIPAWGGAETLY	1.01						

Red: Shared clones in all three 2019 samples;

Blue: Shared clones in two 2019 samples;

Black: Unique clones in each samples.